Supporting Information for

Engineered nanomaterial transformtion under oxidative environmental conditions: Development of an *in vitro* biomimetic assay

Kevin M. Metz[†,1], Andrew N. Mangham,[2] Matthew J. Bierman,[2] Song Jin[2], Robert J. Hamers[2], and Joel A. Pedersen[,1,3]*

[1] Environmental Chemistry and Technology Program, [2]Department of Chemistry, and

[3]Department of Soil Science, University of Wisconsin, Madison, WI 53706

*Corresponding author address: Department of Soil Science, University of Wisconsin, 1525 Observatory Drive, Madison, WI 53706-1299; phone: (608) 263-4971; fax: (608) 265-2595; e-mail: japedersen@soils.wisc.edu.

[†] Present address: Department of Chemistry, Albion College, 611 E. Porter Street, Albion, MI 49224.

solution) exposed to oxidizing solutions.

Figure S13. ICP-OES Zn metal data for filtered QD-PEG$_{350}$ conjugates following oxidative treatment and particle separation.

Text S4. Literature cited

Text S1. Supporting Information for Materials and Methods

Chemicals. Cadmium oxide (99.5%), trioctylphosphine oxide (TOPO, technical grade, 90%), trioctylphosphine (TOP, technical grade, 90%), zinc stearate (technical grade), sulfur powder (99.98%), selenium powder (100 mesh, >99.5%) and tetramethylammonium hydroxide solution (TMAH, ~2.2 M) in methanol were purchased from Sigma-Aldrich Chemicals (Milwaukee, WI). Methoxy-terminated mercapto-polyethylene glycol with a molecular mass of 350 Da (mPEG-thiol, PEG_{350}) was purchased from Diagnostic Chemicals Limited (Charlottetown, PE, Canada). Methoxy-terminated mercapto-polyethylene glycol with a molecular mass of 5000 Da (PEG_{5000}) was purchased from RAPP Polymere (Tübingen, Germany). 2-Methoxy hydroquinone (97%) and *n*-tetradecylphosphonic acid (TDPA, 97%) were purchased from Alfa Aesar (Ward Hill, MA). Ferrous sulfate (ACS Certified), sodium acetate and L-ascorbic acid were purchased from Fisher Scientific (Waltham, MA). 3-*N*-morpholinopropanesulfonic acid (MOPS) sodium salt (98%) was purchased from Acrōs Organics (Geel, Belgium). All powders were used as received and stored under ambient conditions. All aqueous solutions were made with distilled and deionized water (ddH_2O) with a resistivity $\geq$ 18 MΩ-cm.

Synthesis of $CdSe_{core}/ZnS_{shell}$ Quantum Dots. $CdSe_{core}/ZnS_{shell}$ QDs were prepared using a modification of a published procedure(1). In a typical synthesis, 0.25 g CdO, 3 g TOPO, and 0.9 g TDPA were combined in a 25-mL 3-neck flask and heated to 320°C under Ar with stirring until the solution turned clear and colorless. The temperature was reduced to 220°C, and a solution containing 0.19 g Se in 2 mL TOP was rapidly injected. The mixture was allowed to react for 20-30 min until the desired diameter CdSe nanocrystal was formed as determined by UV-Visible spectroscopy (2). The reaction was quenched by addition of a small amount of room

temperature TOP. This CdSe core solution was cooled to near room temperature, then transferred to a 100-mL 3-neck flask. A shell solution was prepared by mixing 4.9 g Zn stearate, 0.125 g S and 30 mL TOP in a round bottomed flask and heating to 110°C under Ar with stirring until a milky white solution was formed in ~30 min. The core solution was heated to 180°C under Ar with stirring, and the shell solution was slowly injected. After a few hours, the mixture was cooled to 110°C and left to incubate overnight. The final solution was cooled to near room temperature and thinned with ~25 mL of toluene. Methanol was added to flocculate the nanocrystals. Quantum dots were isolated by centrifugation. To remove excess coordinating ligands, the isolated product was suspended in toluene, flocculated with methanol and isolated as above. This process constitutes a single wash cycle. The quantum dots used here were washed at least five times in either toluene or chloroform. The final product was stored in a mud state with chloroform.

Functionalization of Quantum Dots. Surface modification of quantum dots was achieved using a ligand exchange process (3-5). We used mPEG-thiol of two molecular masses to replace the coordinating ligands that decorated the surface after synthesis. Many ligand exchanges processes are performed in an organic solvent such as chloroform, driven by mass action (using a large excess of the desired ligand), and completed in a few hours (3-5). Such processes result in low yields of PEG-thiol-terminated $CdSe_{core}/ZnS_{shell}$ quantum dots. To increase yield of water-stable quantum dots, we raised solution pH to ≥ 12, elevated reaction temperature to 42°C, and extended the reaction time to 3 d to facilitate increased thiol binding (3-5). In a typical functionalization, a small amount of quantum dot mud was suspended in chloroform. The quantum dot number concentration was determined by UV-Visible absorption spectroscopy (2). mPEG-thiol was added to achieve a molar concentration 100-fold higher than

the QD number concentration. Solution pH was adjusted to ≥12 by adding 4-5 drops of 1 M tetramethylammonium hydroxide (5) solution in methanol. The solution was shaken for 3 d on an incubating shaker at 150 rpm at 42°C. The solution was diluted to twice its volume with methanol resulting in flocculation of the non-polar components. The mixture was centrifuged, the supernatant containing the quantum dots was poured into a beaker, and the solvent was allowed to evaporate overnight. The dried quantum dots were suspended in ddH_2O by vortexing and filtered through a 0.45-μm syringe filter to remove any aggregated QDs. Water-stable QD suspensions were made by this process with up to 90% recovery of the starting quantum dots. Removal of excess PEG from stock suspensions was achieved by centrifuging the solutions through centrifugal concentrators at ~3,000g for 15-30 min, to separate the quantum dots from the excess ligand. At least three washes of the stock solutions were performed, and PEG removal was monitored by analyzing the collected filtrates by attenuated total reflectance-Fourier transform infrared spectrometry. The stability of the QD suspensions as a function of solution pH was analyzed using pseudo-steady titration (5), Figure S2.

Assay Application. To utilize the assay, we exposed PEGylated QDs to reductant-assisted Fenton's reaction (200 μM H_2O_2 + 20 μM Fe^{2+} + 20 μM reductant). Stock solutions (1 mM) were prepared and purged with Ar prior to use. Reaction solutions were prepared in aluminum foil-wrapped 20-mL glass reaction vials, or 5-mL plastic vials. All glassware was washed with phosphate-free detergents and ddH_2O prior to use. Reaction vials were purged with Ar as the reaction solutions were added. The final volume of the reaction solution was 2 mL and consisted of 2 μM QDs, 200 μM H_2O_2, 20 μM Fe, 20 μM reductant and 10 mM buffer. We generally added the reactants in the following order: QDs, buffer, Fe, reductant, H_2O_2. Variations in the order, however, produced no change in the observed results. The reaction vials were sealed

with Parafilm, agitated briefly by hand, and stored overnight (16-18 h) in the dark, after which time the reaction mixtures were characterized. In addition to Ar purged solutions, experiments were performed in aerobic (ambient conditions), and results did not differ statistically .

Characterization of Reactants and Products. *UV-Visible spectrophotometry* was used to determine the quantum dot core diameter and to measure the quantum dot number concentration (2). Data were collected with a Shimadzu PC-2401 UV-Visible spectrophotometer. The precision of UV-Vis measurements was determined by making triplicate measurements on multiple samples.

X-ray photoelectron spectroscopy was used to verify the presence of the zinc sulfide shell on the CdSe core nanoparticles. Spectra were collected under ultrahigh vacuum ($P < 4 \times 10^{-10}$ Torr) using a monochromatic Al K_α X-ray source (1486.6 eV) and a hemispherical analyzer with a multichannel detector (resolution 0.1-0.2 eV). Data were collected at 45° photoelectron takeoff angles for all spectra. Samples were prepared by drying a chloroform or toluene suspension of quantum dots on a silicon substrate to form a thin QD film. $CdSe_{core}$ samples (i.e., QDs lacking the ZnS shell) were used as controls. The absence of a peak in the Zn $2p_{3/2}$ region of the spectra near 1022 eV confirms that zinc was not present in control samples. Core/shell particles synthesized using the above procedure showed intensity in zinc $2p_{3/2}$ region, verifying the presence of Zn in our $CdSe_{core}/ZnS_{shell}$ samples.

Attenuated total reflectance-Fourier transform infrared spectroscopy was used to characterize initial surface functionalization. Measurements were performed in aqueous suspensions using a Varian FTS 7000 with 500 co-added scans at 4 cm^{-1} resolution collected with a DTGS detector, using a 3-bounce diamond ATR element (MIRacle, Pike Technologies, Madison, WI).

External reflectance-Fourier transform infrared spectroscopy was used to confirm the presence of PEG on QDs that had been exposed to buffer solutions as pH 4.1. Measurements consisted of 50 scans co-added, at 4 cm^{-1} resolution collected on a Bruker Vertex 70 FTIR. QD-PEG_{350} conjugates were suspended overnight in 10 mM acetate buffer at pH 4.1. After 24 h, concentrated HCl was added to the samples to protonate acetate anions. Samples were then drop cast onto highly doped (0.008 ohm-cm) <111> Si at 95 °C. The acetic acid and water was allowed to evaporate, and spectra were collected and referenced against a buffer control prepared the same way.

Transmission Electron Microscopy (TEM) was used to characterize the quantum dots before and after exposure to the MHQ-driven Fenton's reagent. Images were collected on a Philips CM200 TEM operated at 200 kV. Samples were prepared by removing QDs from suspension by 15- to 20-min filtration through a Millipore centrifugal concentrator (regenerated cellulose, 10 kDa nominal molecular weight cutoff (MWCO)) at 3000*g*. Retentates were suspended in a 50:50 ddH_2O:ethanol solution, dispersed dropwise onto lacey carbon-coated Cu TEM grids and allowed to evaporate.

Dynamic light scattering (DLS) was used to estimate the hydrodynamic radii of PEGylated quantum dots in suspension, as well as to evaluate changes in hydrodynamic size following exposure to (reductant-assisted) Fenton's reaction and control solutions. Measurements were performed on a Malvern Zetasizer Nano-ZS and number-average values were reported. Each sample was measured in triplicate, with each measurement reporting the average of 10 runs.

Fluorescence emission spectroscopy was used to examine changes in QD emission upon exposure to solutions used in this study. Data were collected on an ISS PC1 spectrofluorometer

outfitted with a 300 W Xe arc lamp source using 2-nm slits on the excitation and emission monochrometers and an excitation wavelength of 400 nm.

Inductively coupled plasma-optical emission spectroscopy was used to measure Cd and Zn released from quantum dots following the treatments described above. At the conclusion of reactions, nanoparticles were separated from solution by 90-min centrifugation at 3000*g* through a Millipore centrifugal concentrator composed of regenerated cellulose, with a 10 kDa nominal MWCO prior to ICP-OES analysis of the retentate and filtrate. The manufacturer determined the MWCO of the filter by 95% retention of globular proteins of known size and reported that mathematical modeling indicated that the 10 kDa MWCO corresponds to a nominal pore diameter of 2.8 nm. The PEG_{350}- and PEG_{5000}-QDs had diameters of ~6.5nm and ~14 nm [core diameter = 2.6 ± 0.1 nm (as determined by UV-Visible absorption spectroscopy (2)), ZnS shell thickness < 1 nm (XPS), extended PEG_{350} and PEG_{5000} ligand lengths of 1 nm and 4.5 nm] and DLS measurements indicate aggregates in excess of 25 nm. Thus, unless disaggregated and severely degraded, the quantum dots would not pass the filter. The filter geometry was such that 20 μL was retained above the filter in all cases, leading to a small bias in the measured quantities. Prior to analysis, the filtrate and retentate were diluted to 10 mL with ddH_2O, and pH was adjusted to ≤ 2 with 1 M H_2SO_4 or HNO_3. Measurements were taken in triplicate at each wavelength (214.439 nm, 226.502 nm and 228.802 nm for Cd; 202.548 nm, 206.200 nm and 213.857 nm for Zn) using a Varian Vista-MPX ICP-OES with an axial-configured torch alignment. Results at each wavelength were averaged, and the means were reported.

Psuedo-steady state titration was used to examine the solution stability of the PEG_{350}- and PEG_{5000}-QDs as a function of solution pH, as described in detail previously (5). Briefly, aliquots of QD stock solutions were added to water samples that had been pH adjusted, covering

the range of pH 1 to 8. These solutions were allowed to sit overnight, to reach equilibrium, and the optical density of the solutions was measured using UV-Visible spectroscopy. The results of these measurements, Figure S2, were used assess QDs stability in pH range of the designed assay.

Wavenumber (cm^{-1})	Assignment
2935s	CH_3 Asymmetric Stretch
2856	EG-CH_2 stretch broad
2181s	Alky CH_2 stretch
1452	EG-CH_2 scissor
1350	EG-CH_2 wag
1294	EG-CH_2 twist
1246	EG-CH_2 twist
1199	EG-OCH_3 rocking
1140	C-O, C-C Stretch
1095	C-O, C-C Stretch
1028	C-O, C-C Stretch
945	EG-CH_2 rocking

Table S1. Vibrational peak assignments for poly(ethylene glycol) bound to a surface. Compiled from ref (6).

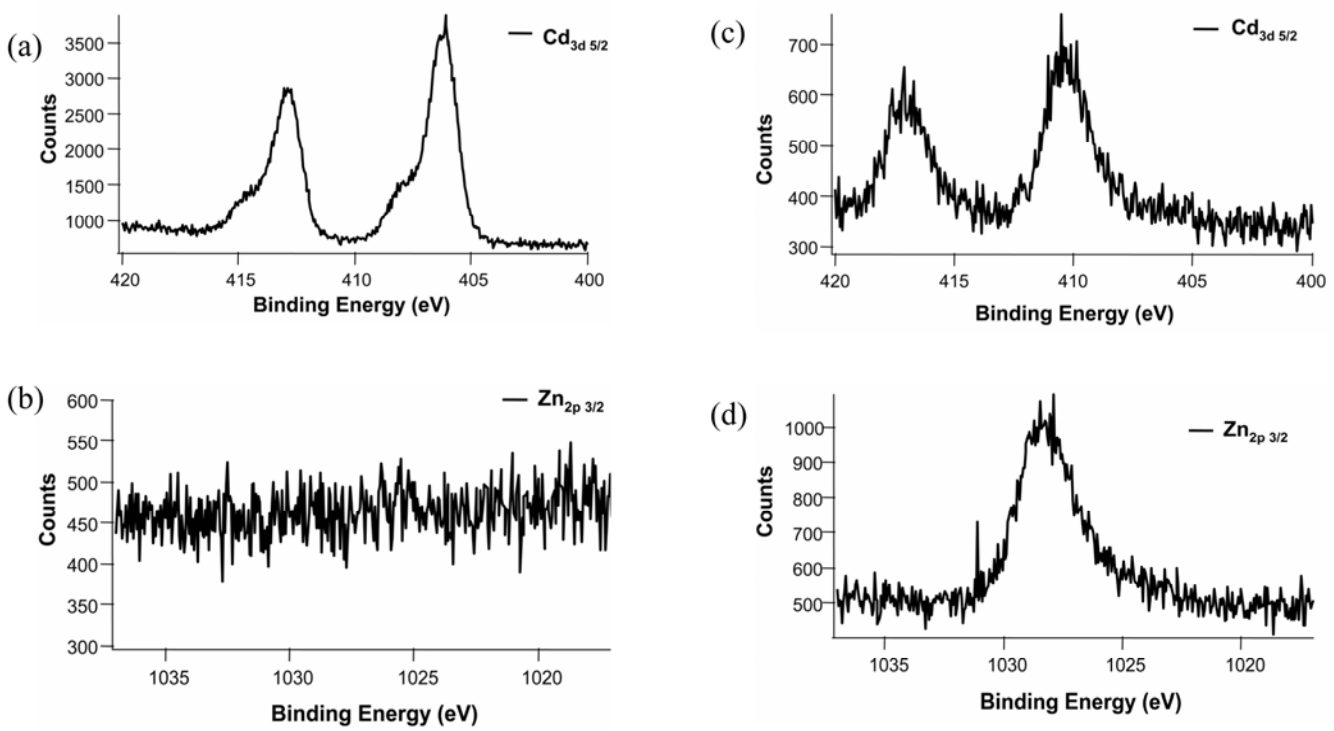

Figure S1. XPS spectra of the Cd $3d_{5/2}$ and Zn $2p_{3/2}$ regions for CdSe QDs (a, b) and $CdSe_{core}/ZnS_{shell}$ QDs (c, d).

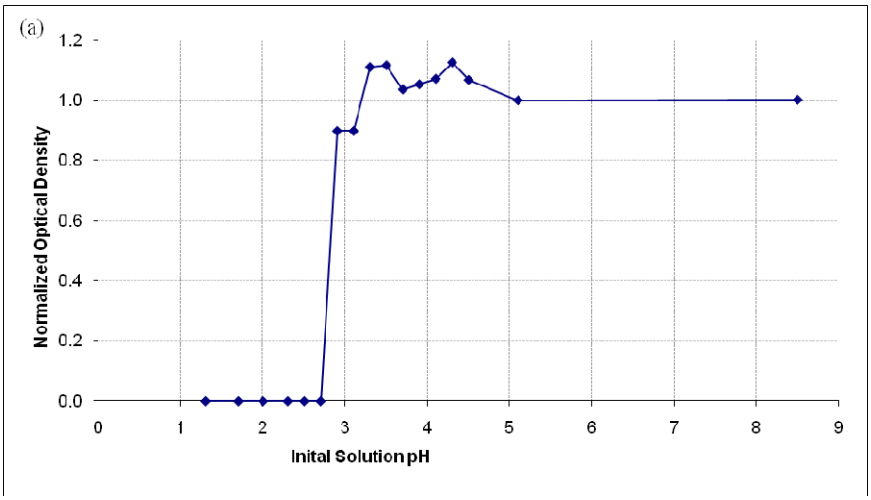

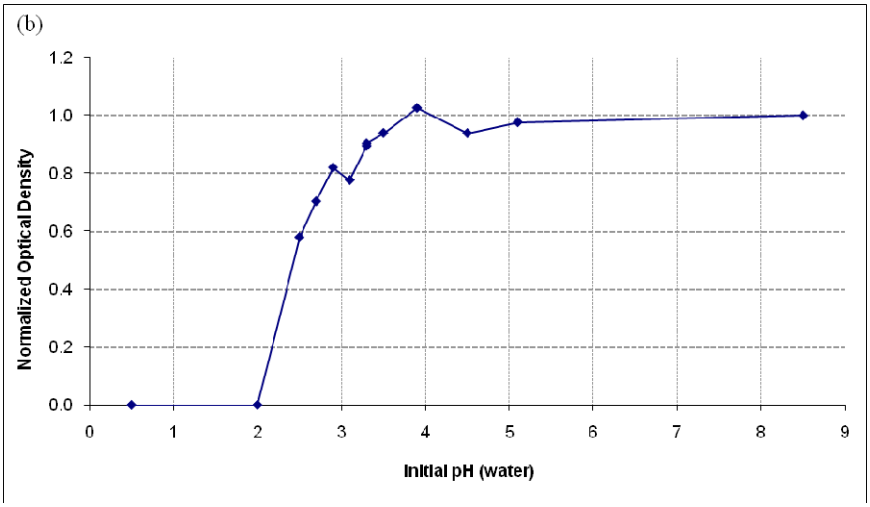

Figure S2. Pseudo-steady state titrations (*5*) of (a) QD-PEG_{5000} and (b) QD-PEG_{350} conjugates, to examine the pH stability of the QD solutions and to select the pH for the MHQ-Fenton assay. The magnitude of first exciton peaks (optical density) were normalized to the first exciton peak of the stock solution at storage pH 8.2. The optical density provides a measure of QD concentration. Loss of PEG from the QD surface would result in aggregation and sedimentation, manifested as a decrease in optical density. For both PEG_{5000} and PEG_{350}, optical density did not significantly change as a function of pH between pH 4 and 9. A sharp decrease in optical density was observed around pH 3. This indicates that pronounced loss of PEG ligand did not occur until pH dropped below 3.4. The MHQ-Fenton assay was conducted at pH 4.1.

(a)

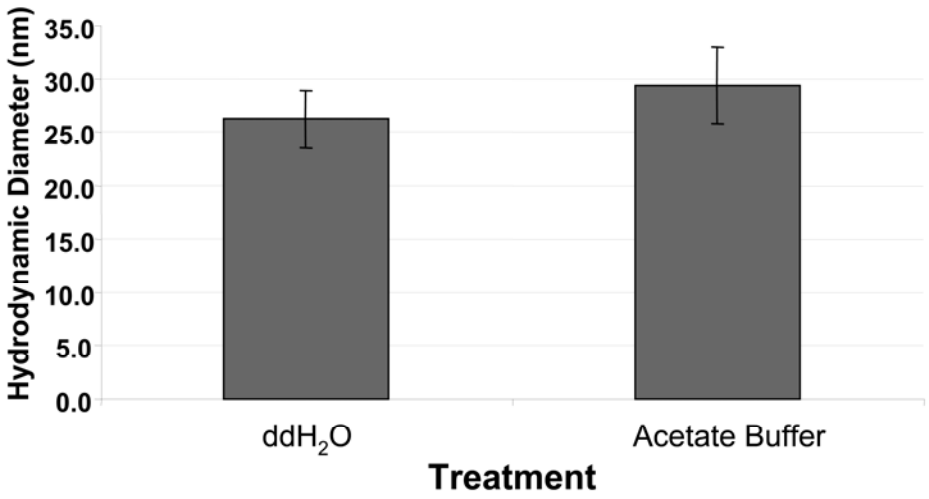

(b)

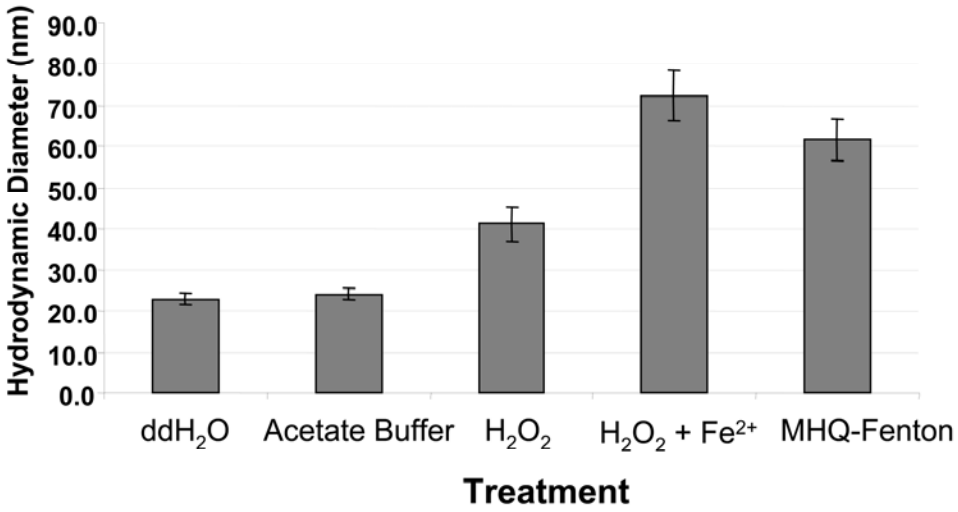

Figure S3. Number-averaged hydrodynamic diameter, determined using dynamic light scattering. Bars represent mean number averaged values for (a) PEG_{350}-QD in ddH_2O and 10 mM acetate buffer and (b) PEG_{5000}-QDs in ddH_2O, 10 mM acetate buffer, 200 μM H_2O_2, 200 μM H_2O_2 + 20 μM Fe^{2+} and the methoxyhydroquinone-driven Fenton's reagent described in the text. Error bars represent one standard deviation.

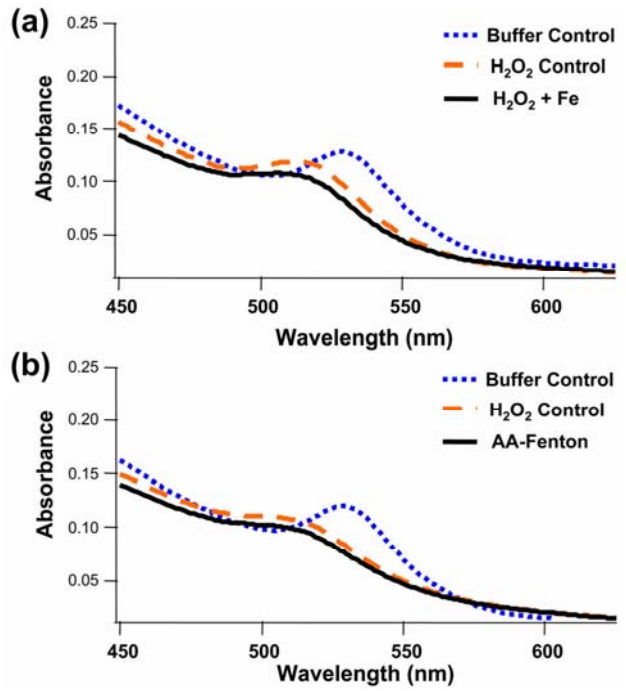

Figure S4. UV-Visible absorption spectra of PEG_{5000}-QDs exposed to (a) classic Fenton's reagent (Fe^{2+} + H_2O_2), and (b) ascorbic acid-driven Fenton's reagent. All reactions were conducted in 10 mM acetate buffer (pH 4.1). The solid black lines represent PEG_{5000}-QDs in the respective Fenton's reagents. The blue dotted lines represent the PEG_{5000}-QDs control in acetate buffer. The orange dashed line represents the PEG_{5000}-QDs in H_2O_2

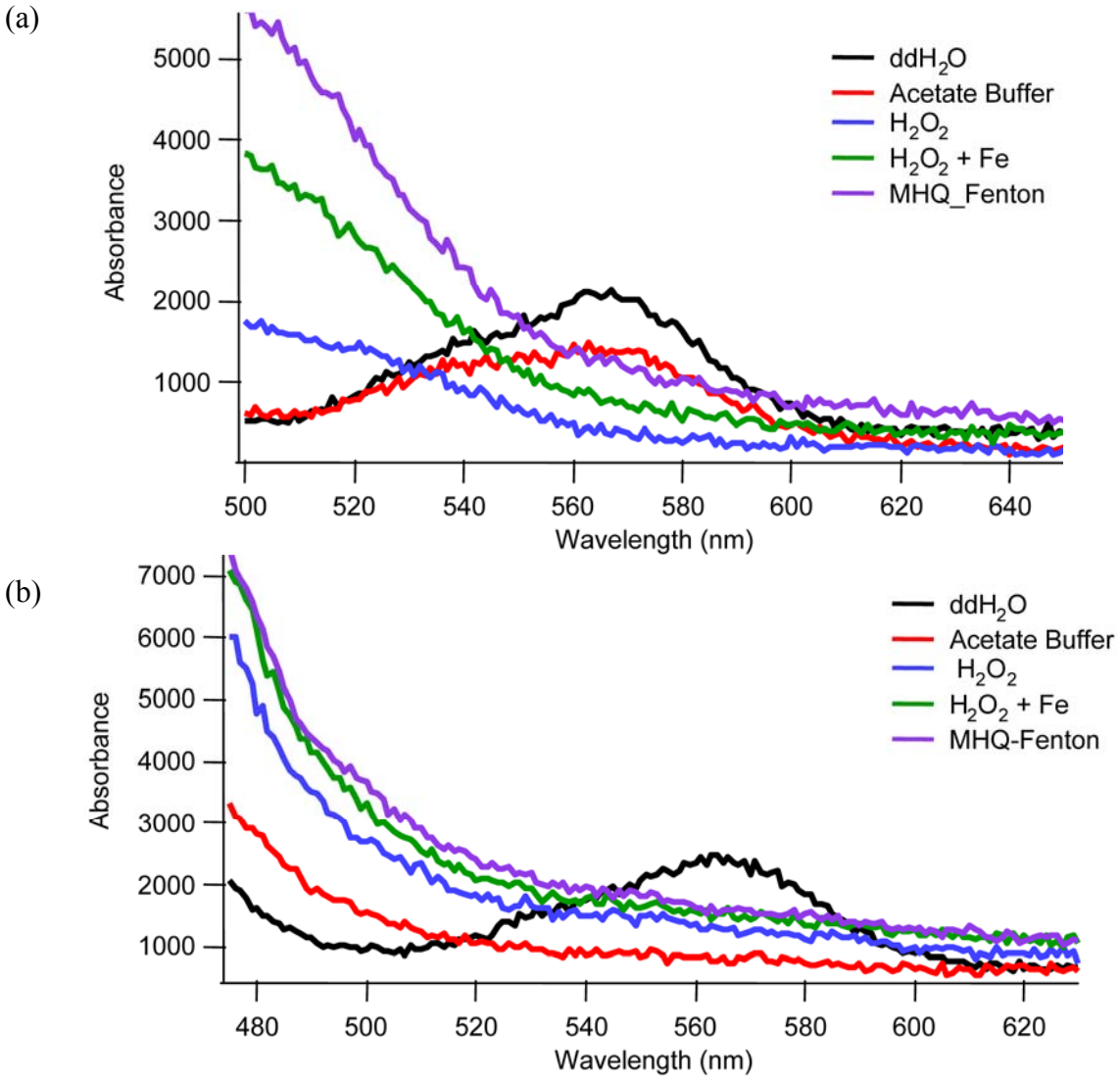

Figure S5. Florescence emission spectra of (a) PEG_{5000}-QDs and (b) PEG_{350}-QDs exposed to acetate buffer, H_2O_2, H_2O_2 + Fe^{2+} and the MHQ-driven Fenton's reaction. In these spectra an emission peak at 560 nm was observed in ddH_2O and 10 mM acetate buffer. Upon exposure to H_2O_2 this peak diminished in intensity. The peak nearly disappeared following exposure to the classical Fenton's reagent and was indistinguishable from background following exposure to MHQ-Fenton reagent. These measurements appeared consistent with those observed from UV-Visible spectroscopy.

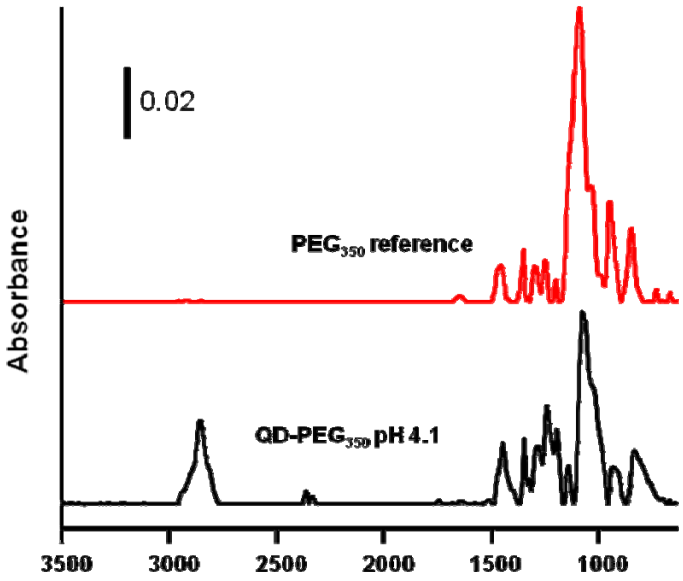

Figure S6. FTIR spectra of PEG_{350} (top, red) and QD-PEG_{350} (bottom, black) after exposure to 10 mM acetate at pH 4.1 for 24 h. Both spectra were referenced a buffer control. The slight shift in QD-PEG_{350} sample peaks was due to differences in the local environment (presence of Cd ions). Nonetheless, the QD-PEG_{350} spectrum clearly corresponds to the PEG_{350} reference sample and confirms the presence of PEG on the particles after 24-h exposure to pH 4.1 conditions.

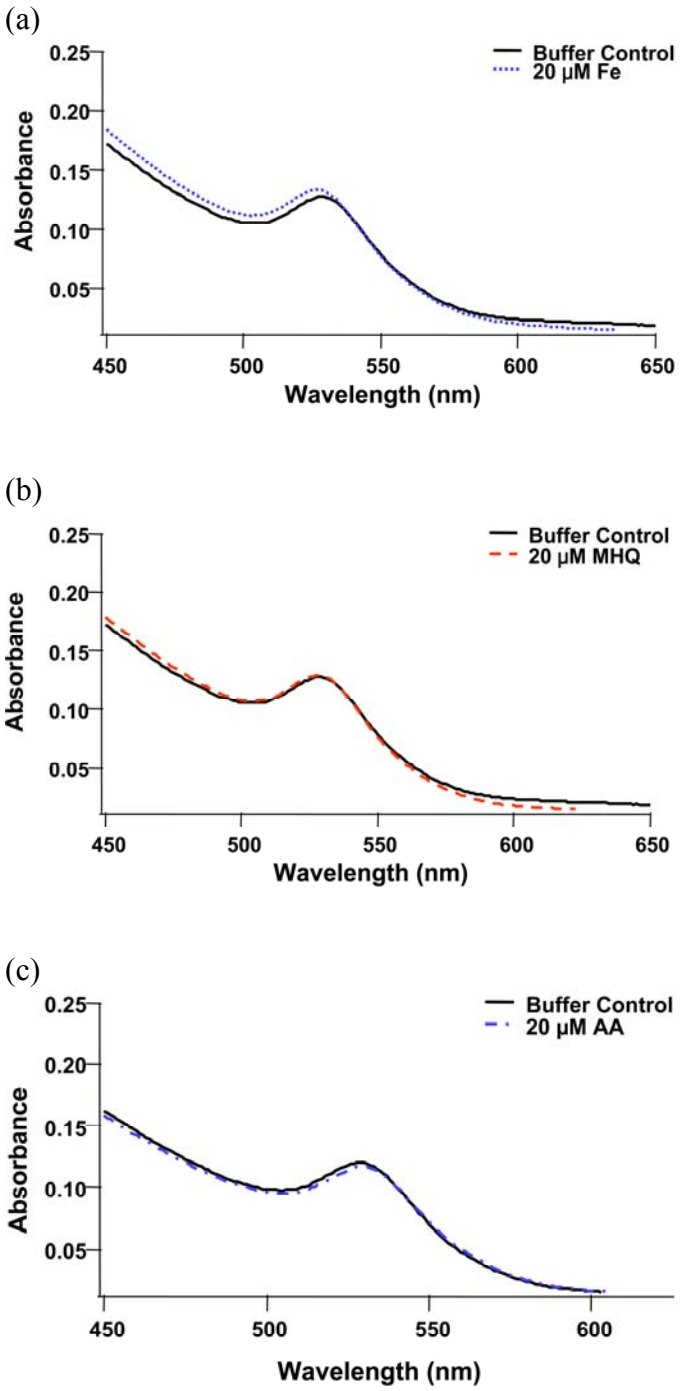

Figure S7. Representative UV-Visible spectra of PEG_{5000}-QDs exposed to single assay components: (a) 20 µM Fe^{2+}, (b) 20 µM MHQ and (c) 20 µM AA, all in 10 mM acetate buffer at pH 4.1. No significant change was observed relative to the PEG_{350}-QD spectra in buffer alone (solid black line in each plot).

(a)

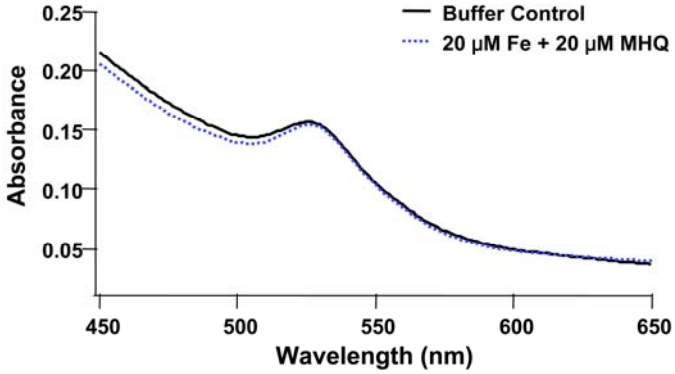

(b)

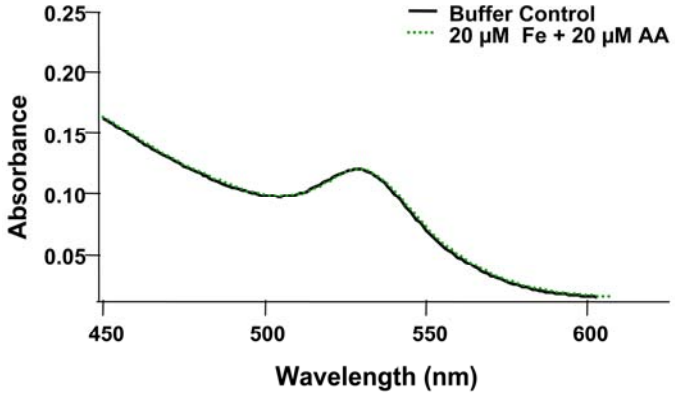

Figure S8. Representative UV-Visible spectra of PEG_{5000}-QDs exposed to binary combinations of assay components: (a) 20 µM Fe^{2+} + 20 µM MHQ and (b) 20 µM Fe^{2+}+ 20 µM AA, in 10 mM acetate buffer at pH 4.1. No significant change was observed relative to the PEG_{5000}-QD spectra in buffer alone.

(a)

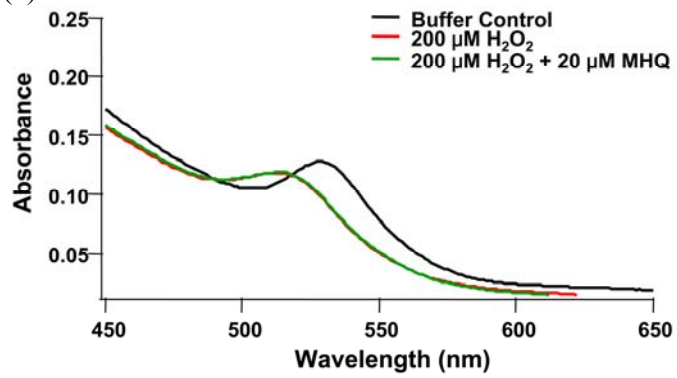

(b)

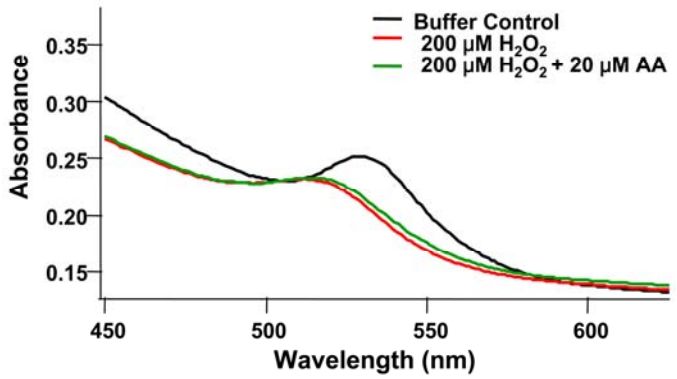

Figure S9. Representative UV-Visible spectra of PEG_{5000}-QDs exposed to binary combinations of assay components: (a) 200 μM H_2O_2 + 20 μM MHQ and (b) 200 μM H_2O_2 + 20 μM AA, in 10 mM acetate buffer at pH 4.1. No significant change was observed relative to the PEG_{5000}-QD spectra exposed to 200 μM H_2O_2 in buffer solution. UV-Visible spectra for PEG_{5000}-QD in buffer shown for comparison.

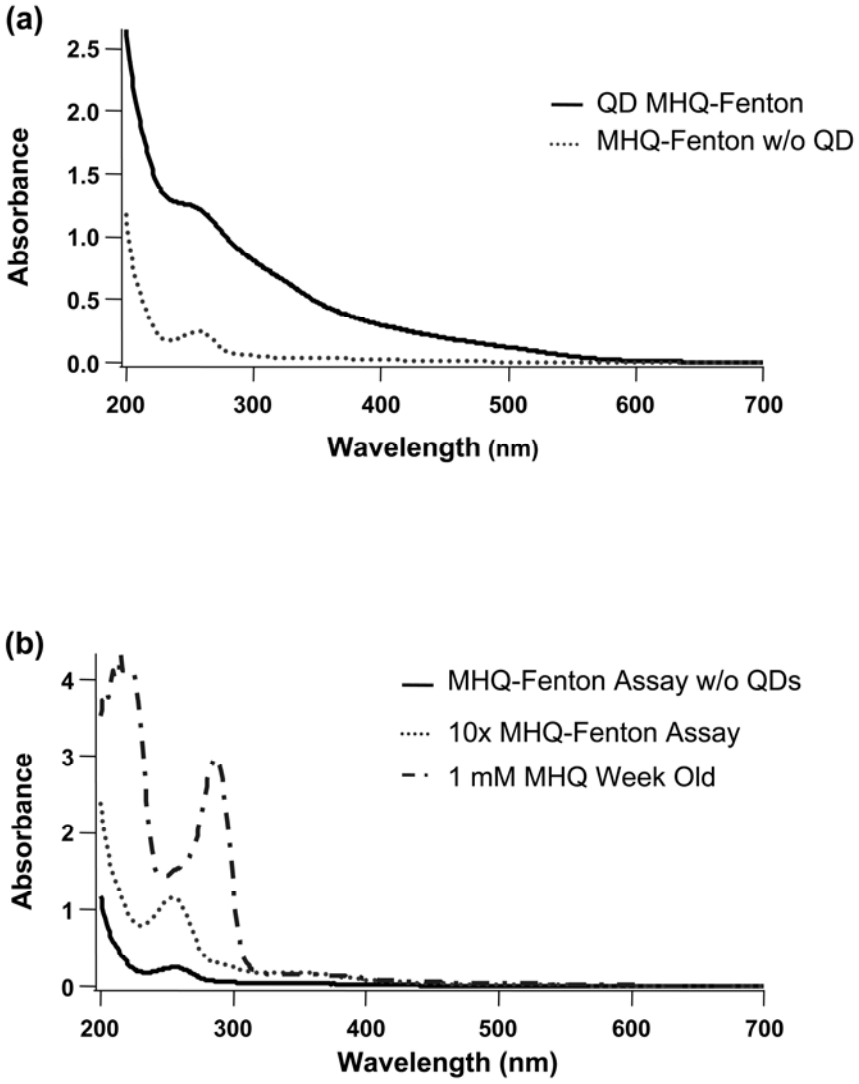

Figure S10. UV-Visible spectra of (a) PEG_{5000}-QDs exposed to the methoxyhydroquinone-driven Fenton's reagent and the reagent without the QDs, demonstrating that the background signal does not arise from the methoxyhydroquinone, and (b) oxidized methoxyhydroquinone of different concentrations. The solid line represents the MHQ-Fenton assay ran overnight without QDs. The dotted line represents the MHQ-Fenton assay components at ten times the concentration used for our studies (viz. 2 mM H_20_2, 200 μM MHQ and 200 μM Fe^{+2}). The dot-dash line is a 1 mM MHQ stock solution after oxidizing for 1 week.

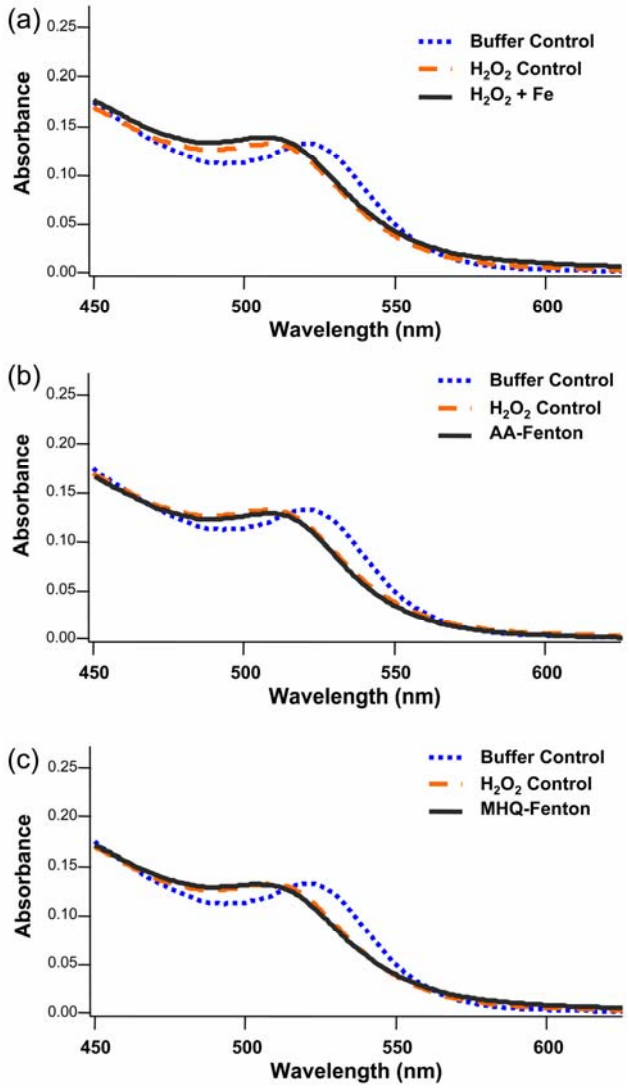

Figure S11. UV-Visible absorption spectra of PEG_{5000}-QDs exposed to (a) Fenton's reagent (H_2O_2 + Fe^{2+}), (b) ascorbic acid (AA)-driven Fenton's reagent, and (c) methoxyhydroquinone (MHQ)-driven Fenton's reagent at pH 6 (10 mM MOPS). Exposure to H_2O_2 caused a 10-nm blue shift in the peak corresponding to the first exciton peak. Addition of Fe^{2+} (and reductants) failed to produce further changes in the spectra.

Text S2. Transformation of PEG_{5000}-QDs by MHQ-Fenton's Reaction at pH 6. We exposed PEG_{5000}-QDs to MHQ-Fenton's reaction at pH 6 (10 mM 3-*N*-morpholinopropanesulfonic acid (MOPS)) to examine the effect of raising assay pH on QD integrity. MOPS was selected for the pH 6 treatment due to the low propensity of this buffer to complex divalent ions in solution (7,8). Figure 5 shows UV-Visible spectra of PEG_{5000}-QDs for

treatments analogous to those in Figure 2 but at pH 6. As in Figure 2, these spectra show increasing absorbance moving from long wavelengths to the characteristic first exciton peak centered near 525 nm followed by a nearly linear absorbance at higher energies. The first exciton peak in the spectrum of the hydrogen peroxide-exposed QDs shows a blue shift relative to the buffer control, with the peak centered ~510 nm and a small decrease in absorbance. Differences between the UV-Visible spectra for each Fenton's reaction (classical Fenton's (Figure 5a), AA-Fenton's (Figure 5b), MHQ-Fenton's reaction (Figure 5c)) and that for H_2O_2-exposed QDs fell within the limits of the experimental uncertainty (± 1 nm wavelength, ± 0.01 abs).

As expected, addition of Fe^{2+} (with or without an organic reductant) to H_2O_2 at pH 6 failed to increase degradation of PEG_{5000}-QDs. Fenton's reaction is most effective in degrading organic environmental contaminants at low pH (viz. pH 3) with a steady decrease in activity as pH rises (e.g. Fenton's reaction is two orders of magnitude slower at pH 5 compared to pH 3) (9,10). Additionally, as pH increases toward neutral, Fe^{III} speciation is increasingly dominated by $Fe(OH)_{3(s)}$ formation (11), reducing the concentration of ferrous iron in solution, and lowering the hydroxyl radical generation by Fenton's reagent. The immediate extracellular environment of lignolytic fungi is typically acidic (pH 3-5) (12). Use of low pH in the assay simulates environmental conditions where ferrous iron is stable and Fenton's chemistry is enabled, resulting in higher $^{\bullet}OH$ production. The lack of change in the QD core size at higher pH values is also consistent with previous observations that the ZnS shell provides a barrier to oxidation in biological media at circum neutral pH (13).

Text S3. Effect of Excess Ligand on Oxidative Stability

Initial experiments with PEG_{350}-thiol ligands appeared to suggest that shorter chain length ligands offer improved stability to oxidation relative to the bulkier PEG_{5000}-thiol ligands.

Figure 4a in the main text shows the UV-Visible spectrum for PEG_{350}-QDs exposed to MHQ-Fenton's reagent, H_2O_2 and buffer alone. As expected, the buffer control spectrum exhibited increasing absorption from long wavelengths to the first exciton peak, centered near 515 nm (corresponding to CdSe core diameters of 2.5 ± 0.1 nm), followed by a nearly linear increase in absorbance at shorter wavelengths. Upon exposure of PEG_{350}-QDs to H_2O_2, the spectrum retained a similar shape, with a slight blue shift to ~510 nm and a small (~9%) decrease in amplitude. Exposure of PEG_{350}-QDs to the MHQ-Fenton's reaction yielded dots producing an absorption spectrum with a shape and first exciton peak energy indistinguishable from those for H_2O_2-exposed QDs. Results similar to the H_2O_2-exposure were obtained for both the classical and AA-driven Fenton's reactions (data not shown).

In these initial experiments with PEG_{350}-QDs, production of the stronger oxidant $^{\bullet}OH$ produced no further discernable change in CdSe core size or concentration beyond that produced by H_2O_2. Protection of QDs from photooxidation by excess ligand in solution has been reported (14). We hypothesized that excess ligand in solution may have protected the PEG_{350}-QDs from oxidation by (reductant-assisted) Fenton's reaction by scavenging hydroxyl radicals, preventing them from attacking the QDs.

The presence of excess ligand in solution can dramatically influence extent of QD degradation by MHQ-Fenton's reagent and H_2O_2. Our results imply that excess ligand compete with PEGylated QDs for oxidants and that longer chain length PEG provides a more effective barrier against the oxidants H_2O_2 and $^{\bullet}OH$. Similar effects of ligand chain length have been observed in photo-oxidation experiments: water-stable ligands (e.g., disulfides of long aliphatic ligands) keep QD cores dispersed in solution as the cores were oxidized (14). In contrast,

complete oxidation of the QD core was observed with shorter, less stable ligands, such as aromatic thiols (14).

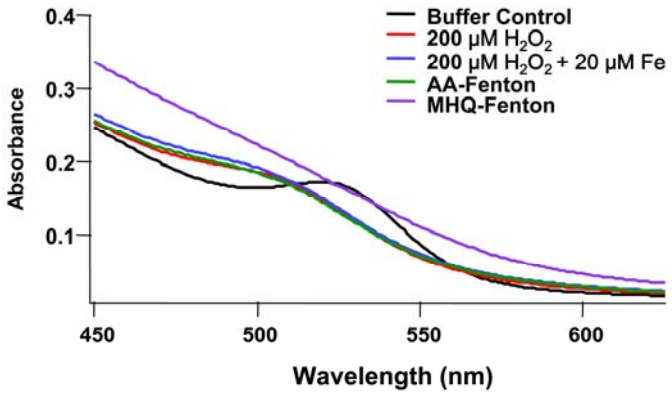

Figure S12. UV-Visible spectra of PEG_{5000}-QDs filtered to remove excess ligand from solution and exposed to various oxidizing solutions.

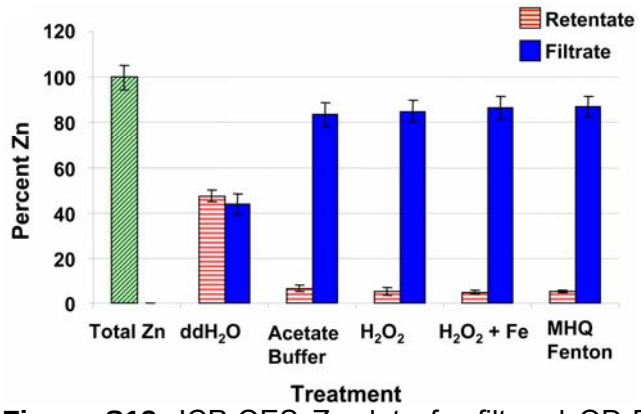

Figure S13. ICP-OES Zn data for filtered QD-PEG_{350} following various oxidative treatments. Similar to QD-PEG_{5000} results, Zn was present in both the filtrate and retentate for each solution. The Zn concentration in the retentate decreased gradually from 47 ± 3 % for the ddH_2O to 5.1 ± 0.6 % for the MHQ-Fenton's reaction. Recovery of total zinc was ≥90 %; total Zn concentrations do not differ between the control and any of treatments ($p \geq 0.05$). Inclusion of the ddH_2O control allowed verification that PEG_{350} was a poor protective barrier and permitted the oxidation of the ZnS shell in acidic buffer media as hypothesized above. The presence of Zn in the filtrate for the filtered PEG_{350}-QD sample in ddH_2O could be the result of a dynamic monolayer, or de-PEGylation at low QD concentrations as discussed above.

Text S4. Literature Cited

(1) Huang, G. W.; Chen, C. Y.; Wu, K. C.; Ahmed, M. O.; Chou, P. T., One-pot synthesis and characterization of high-quality CdSe/ZnX (X = S, Se) nanocrystals via the CdO precursor. *J. Crystal Growth* **2004**, *265*, 250-259.

(2) Yu, W. W.; Qu, L. H.; Guo, W. Z.; Peng, X. G., Experimental determination of the extinction coefficient of CdTe, CdSe, and CdS nanocrystals. *Chem. Mater.* **2003**, *15*, 2854-2860.

(3) Kang, E. C.; Ogura, A.; Kataoka, K.; Nagasaki, Y., Preparation of water-soluble PEGylated semiconductor nanocrystals. *Chem. Lett.* **2004**, *33*, 840-841.

(4) Chan, W. C. W.; Nie, S. M., Quantum dot bioconjugates for ultrasensitive nonisotopic detection. *Science* **1998**, *281*, 2016-2018.

(5) Aldana, J.; Lavelle, N.; Wang, Y. J.; Peng, X. G., Size-dependent dissociation pH of thiolate ligands from cadmium chalcogenide nanocrystals. *J. Am. Chem. Soc.* **2005**, *127*, 2496-2504.

(6) Harder, P.; Grunze, M.; Dahint, R.; Whitesides, G. M.; Laibinis, P. E., Molecular conformation in oligo(ethylene glycol)-terminated self-assembled monolayers on gold and silver surfaces determines their ability to resist protein adsorption. *J. Phys. Chem. B* **1998**, *102*, 426-436.

(7) Perrin, D. D.; Dempsey, B. *Buffers for pH and Metal Ion Control*; John Wiley & Sons: New York, 1974.

(8) Zhang, H. C.; Huang, C. H., Oxidative transformation of fluoroquinolone antibacterial agents and structurally related amines by manganese oxide. *Environ. Sci. Technol.* **2005**, *39*, 4474-4483.

(9) Burbano, A. A.; Dionysiou, D. D.; Suidan, M. T.; Richardson, T. L., Oxidation kinetics and effect of pH on the degradation of MTBE with Fenton reagent. *Wat. Res.* **2005**, *39*, 107-118.

(10) Duesterberg, C. K.; Waite, T. D., Process optimization of Fenton oxidation using kinetic modeling. *Environ. Sci. Technol.* **2006**, *40*, 4189-4195.

(11) Stumm, W.; Morgan, J. J. *Aquatic Chemistry*; 3rd ed.; John Wiley & Sons, INC.: New York, 1996.

(12) Wood, P. M., Pathways Of production of Fenton reagent by wood-rotting fungi. *FEMS Microbiol. Rev.* **1994**, *13*, 313-320.

(13) Medintz, I. L.; Uyeda, H. T.; Goldman, E. R.; Mattoussi, H., Quantum dot bioconjugates for imaging, labelling and sensing. *Nature Mater.* **2005**, *4*, 435-446.

(14) Aldana, J.; Wang, Y. A.; Peng, X. G., Photochemical instability of CdSe nanocrystals coated by hydrophilic thiols. *J. Am. Chem. Soc.* **2001**, *123*, 8844-8850.